Journal of Solid Mechanics Vol. 10, No. 2 (2018) pp. 232-248

Wave Propagation Analysis of CNT Reinforced Composite Micro-Tube Conveying Viscose Fluid in Visco-Pasternak Foundation Under 2D Multi-Physical Fields

A.H. Ghorbanpour Arani [1, *], M.M. Aghdam [1], M.J. Saeedian [2]

[1] *Faculty of Mechanical Engineering, Amirkabir University of Technology, Hafez Avenue, Tehran, Iran*
[2] *Faculty of Mechanical Engineering, University of Kashan, Kashan, Iran*

Received 19 January 2018; accepted 22 March 2018

ABSTRACT

In this research, wave propagation analysis in polymeric smart nanocomposite micro-tubes reinforced by single-walled carbon nanotubes (SWCNT) conveying fluid is studied. The surrounded elastic medium is simulated by visco-Pasternak model while the composite micro-tube undergoes electro-magneto-mechanical fields. By means of micromechanics method, the constitutive structural coefficients of nanocomposite are obtained. The fluid flow is assumed to be incompressible, viscous and irrotational and the dynamic modelling of fluid flow and fluid viscosity are calculated using Navier-Stokes equation. Micro-tube is simulated by Euler-Bernoulli and Timoshenko beam models. Based on energy method and the Hamilton's principle, the equation of motion are derived and modified couple stress theory is utilized to consider the small scale effect. Results indicate the influences of various parameters such as the small scale, elastic medium, 2D magnetic field, velocity and viscosity of fluid and volume fraction of carbon nanotube (CNT). The result of this study can be useful in micro structure and construction industries.

Keywords: Waves; Beams; Fibre reinforced composites; Piezoelectricity; Fluid dynamics; Magnetic field.

1 INTRODUCTION

COMPOSITE materials are engineered or naturally occurring materials made from two or more constituent materials with significantly different physical or chemical properties which remain separate and distinct within the finished structure. Most composites have strong, stiff fibres in a matrix which is weaker and less stiff. The objective is usually to make a component which is strong and stiff, often with a low density. Fiber-reinforced polymer (FRP) is a composite material made of a polymer matrix reinforced with fibers and commonly used in the aerospace, automotive, marine, and construction industries [1]. Many previous studies with respect to the wave propagation behavior have been carried out using different models. Dong et al. [2] studied the wave propagation in multi-walled carbon nanotubes (MWCNTs) embedded in a matrix material. Their results showed that the surrounding elastic matrix increased the threshold frequency of wave propagation in the MWCNTs. Wang et al [3] studied the scale effect on wave propagation of double-walled carbon nanotubes (DWCNT). They used Eringen's theory and showed the significance of the small-scale effect on wave propagation in MWCNT. Abdollahian et al [4]

[*] Corresponding author. Tel.: +98 31 55912450; Fax: +98 31 55912424.
E-mail address: gh.amir36@yahoo.com (A.H. Ghorbanpour Arani).

analyzed the non-local wave propagation in embedded armchair triple-walled boron nitride nanotube (TWBNNTs) conveying viscous fluid using differential quadrature method (DQM). Their results showed that by increasing fluid velocity, the phase velocity of wave decreases. Kaviani and Mirdamadi [5] investigated the wave propagation analysis of CNT conveying fluid including slip boundary condition and strain/inertial gradient theory. They showed that the boundary condition between the interface of fluid and structure, plays an important role on the structural response. Ghorbanpour Arani et al [6] studied the nonlocal wave propagation in an embedded double –walled BNNT (DWBNNT) conveying fluid via strain gradient theory. They showed the upstream and downstream wave propagation. Furthermore, they found that the effect of fluid-conveying on wave propagation of the DWBNNT is significant at lower wave numbers. Wave propagation in SWCNT under longitudinal magnetic field using nonlocal Euler–Bernoulli beam theory (EBBT) were analyzed by Narendar et al [7]. Their results showed that the velocity of flexural waves in SWCNTs increases with the increase of longitudinal magnetic field exerted on it in the frequency range; 0–20 THz. Ghorbanpour Arani et al [8] studied the nonlocal piezo elasticity based wave propagation of bonded double-piezoelectric nanobeam-systems (DPNBSs). They obtained phase velocity; cutoff and escape frequencies of the DPNBSs by an analytical method. Reddy and Arbind [9] presented the bending relationships between the modified couple stress-based functionally graded Timoshenko beam theory (TBT) and homogeneous EBBT. They used the modified couple stress for considering the small scale effect. Mosallaie Barzoki et al. [10] studied the Electro-thermo-mechanical torsional buckling of a piezoelectric polymeric cylindrical shell reinforced by DWBNNTs with an elastic core. They utilized representative volume element (RVE) based on micromechanical modeling to determine mechanical, electrical and thermal characteristics of the equivalent composite.

This paper aims to study wave propagation analysis in polymeric smart nanocomposite micro-tubes reinforced by SWCNT conveying fluid flow. In order to control the stability of the system, composite cylinder is subjected to an applied electric and magnetic field while the magnetic field is effective in two direction for the first time. The nanocomposite micro-tube is embedded in a viscoelastic medium which is simulated by visco-pasternak model. The governing equations are derived using Hamilton's principle and solved by applying DQM. The influence of fluid velocity, geometrical parameters of shell, viscoelastic foundation, volume fraction of fiber in polymer matrix, cutoff and escape frequency on the phase velocity of composite cylindrical shell are investigated.

2 MICRO-ELECTROMECHANICAL MODELS FOR COMPOSITES PROPERTIES

A micro-mechanical models known as "XY PEFRC" or "YX PEFRC" is employed for modeling of coupled composite micro-structures. A RVE has been considered for predicting the elastic, piezoelectric and dielectric properties of the smart system. In this research, matrix is assumed to be smart. According to the XY PEFRC micro-mechanical method, the constitutive equations for the electro-mechanical behavior of the selected RVE are expressed as [10]:

$$\begin{bmatrix}\sigma_1\\ \sigma_2\\ \sigma_3\\ \sigma_{23}\\ \sigma_{31}\\ \sigma_{12}\end{bmatrix}=\begin{bmatrix}C_{11} & C_{12} & C_{13} & 0 & 0 & 0\\ C_{12} & C_{22} & C_{23} & 0 & 0 & 0\\ C_{13} & C_{23} & C_{33} & 0 & 0 & 0\\ 0 & 0 & 0 & C_{44} & 0 & 0\\ 0 & 0 & 0 & 0 & C_{55} & 0\\ 0 & 0 & 0 & 0 & 0 & C_{66}\end{bmatrix}\begin{bmatrix}\varepsilon_1\\ \varepsilon_2\\ \varepsilon_3\\ 2\varepsilon_{23}\\ 2\varepsilon_{31}\\ 2\varepsilon_{12}\end{bmatrix}-\begin{bmatrix}0 & 0 & e_{31}\\ 0 & 0 & e_{32}\\ 0 & 0 & e_{33}\\ 0 & e_{24} & 0\\ e_{15} & 0 & 0\\ 0 & 0 & 0\end{bmatrix}\begin{bmatrix}E_1\\ E_2\\ E_3\end{bmatrix}$$

$$\begin{bmatrix}D_1\\ D_2\\ D_3\end{bmatrix}=\begin{bmatrix}0 & 0 & 0 & 0 & e_{15} & 0\\ 0 & 0 & 0 & e_{24} & 0 & 0\\ e_{31} & e_{32} & e_{33} & 0 & 0 & 0\end{bmatrix}\begin{bmatrix}\varepsilon_1\\ \varepsilon_2\\ \varepsilon_3\\ 2\varepsilon_{23}\\ 2\varepsilon_{31}\\ 2\varepsilon_{12}\end{bmatrix}+\begin{bmatrix}\in_{11} & 0 & 0\\ 0 & \in_{22} & 0\\ 0 & 0 & \in_{33}\end{bmatrix}\begin{bmatrix}E_1\\ E_2\\ E_3\end{bmatrix} \quad (1)$$

In this work, Polyvinylidene fluoride (PVDF) is used as a matrix that reinforced by CNT as a fiber. The polymeric piezoelectric fiber reinforced composites (PPFRC) is assumed to be orthotropic and homogeneous with

respect to their principal axes. Coefficients in the above equation in terms of smart matrix and piezoelectric fibers properties and volume fraction of the reinforcement are written as follows [11]:

$$
\begin{aligned}
&C_{11}=\frac{C_{11}^{r}C_{11}^{m}}{\rho C_{11}^{m}+(1-\rho)C_{11}^{r}}\\
&C_{12}=C_{11}\left[\frac{\rho C_{12}^{r}}{C_{11}^{r}}+\frac{(1-\rho)C_{12}^{m}}{C_{11}^{m}}\right]\\
&C_{13}=C_{11}\left[\frac{\rho C_{13}^{r}}{C_{11}^{r}}+\frac{(1-\rho)C_{13}^{m}}{C_{11}^{m}}\right]\\
&C_{22}=\rho C_{22}^{r}+(1-\rho)C_{22}^{m}+\frac{C_{12}^{2}}{C_{11}}-\frac{\rho\left(C_{12}^{r}\right)^{2}}{C_{11}^{r}}-\frac{(1-\rho)\left(C_{12}^{m}\right)^{2}}{C_{11}^{m}}\\
&C_{23}=\rho C_{23}^{r}+(1-\rho)C_{23}^{m}+\frac{C_{12}C_{13}}{C_{11}}-\frac{\rho C_{12}^{r}C_{13}^{r}}{C_{11}^{r}}-\frac{(1-\rho)C_{12}^{m}C_{13}^{m}}{C_{11}^{m}}\\
&C_{33}=\rho C_{33}^{r}+(1-\rho)C_{33}^{m}+\frac{C_{13}^{2}}{C_{11}}-\frac{\rho\left(C_{13}^{r}\right)^{2}}{C_{11}^{r}}-\frac{(1-\rho)\left(C_{13}^{m}\right)^{2}}{C_{11}^{m}}\\
&C_{44}=\rho C_{44}^{r}+(1-\rho)C_{44}^{m}\\
&C_{55}=\frac{A'}{B'^{2}+A'C'}\ ,C_{66}=\frac{C_{66}{}^{r}C_{66}{}^{m}}{\rho C_{66}{}^{m}+(1-\rho)C_{66}{}^{r}}\\
&e_{31}=C_{11}\left[\frac{\rho e_{31}^{r}}{C_{11}^{r}}+\frac{(1-\rho)e_{31}^{m}}{C_{11}^{m}}\right]\\
&e_{32}=\rho e_{32}^{r}+(1-\rho)e_{32}^{m}+\frac{C_{12}e_{13}}{C_{11}}-\frac{\rho C_{12}^{r}e_{31}^{r}}{C_{11}^{r}}-\frac{(1-\rho)C_{12}^{m}e_{31}^{m}}{C_{11}^{m}}\\
&e_{33}=\rho e_{33}^{r}+(1-\rho)e_{33}^{m}+\frac{C_{13}^{r}e_{31}}{C_{11}}-\frac{\rho C_{13}^{r}e_{31}^{r}}{C_{11}^{r}}-\frac{(1-\rho)C_{13}^{m}e_{31}^{m}}{C_{11}^{m}}\\
&e_{24}=\rho e_{24}{}^{r}+(1-\rho)e_{24}{}^{m},e_{15}=\frac{B'}{B'^{2}+A'C'}
\end{aligned}
\tag{2}
$$

where

$$
\begin{aligned}
&A'=\frac{\rho C_{55}{}^{p}}{C_{55}{}^{p}\in_{11}{}^{p}+(e_{15}{}^{p})^{2}}+\frac{(1-\rho)C_{55}{}^{m}}{C_{55}{}^{m}\in_{11}{}^{m}+(e_{15}{}^{m})^{2}}\\
&B'=\frac{\rho e_{15}{}^{p}}{C_{55}{}^{p}\in_{11}{}^{p}+(e_{15}{}^{p})^{2}}+\frac{(1-\rho)e_{15}{}^{m}}{C_{55}{}^{m}\in_{11}{}^{m}+(e_{15}{}^{m})^{2}}\\
&C'=\frac{\rho\in_{11}{}^{p}}{C_{55}{}^{p}\in_{11}{}^{p}+(e_{15}{}^{p})^{2}}+\frac{(1-\rho)\in_{11}{}^{m}}{C_{55}{}^{m}\in_{11}{}^{m}+(e_{15}{}^{m})^{2}}
\end{aligned}
\tag{3}
$$

Superscripts *r* and *m* refer to the reinforced and matrix components of the composite, respectively. ρ is also the volume fraction of the reinforced CNTs in matrix.

3 THE MODIFIED COUPLE STRESS PIEZOELECTRICITY THEORY

Fig. 1 shows a CNT reinforced composite micro-tube embedded in Visco-Pasternak medium. Micro-tube is conveying fluid and undergoes 2D magnetic and electric field simultaneously.

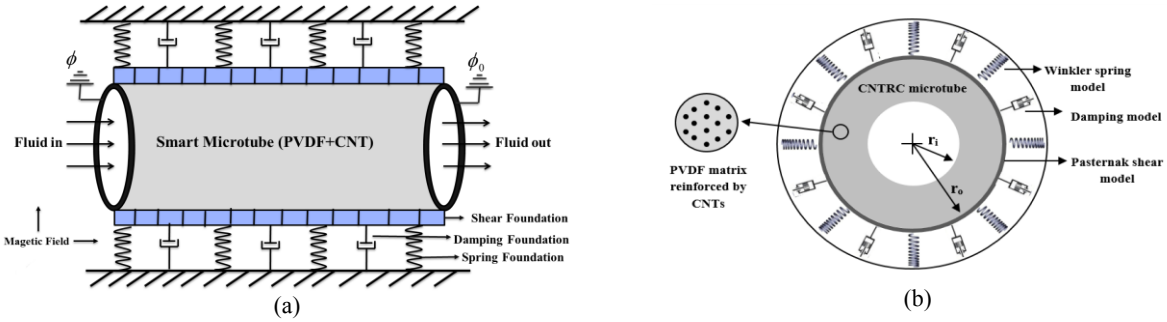

Fig.1
Schematic of a composite micro-tube embedded in Visco-Pasternak medium conveying fluid subjected to electric and magnetic field.

Based on the modified couple stress piezoelectricity theory, the strain energy of an elastic beam can be expressed as [5,9]:

$$U = \frac{1}{2}\int_V \left(\sigma_{ij}\varepsilon_{ij} + m_{ij}\chi_{ij} - D_i E_i\right)dV \tag{4}$$

where σ_{ij} are the components of the symmetric part of the Cauchy stress tensor, D_i are electric displacement components, E_i axial electric field, m_{ij} denote the components of the deviatoric part of the symmetric couple stress tensor, and χ_{ij} are the components of the symmetric curvature tensor which are defined by:

$$E_x = -\frac{\partial \varphi}{\partial x} \tag{5}$$

$$m_{ij} = 2Gl_0^{\,2}\chi_{ij} \tag{6}$$

$$\chi_{ij} = \frac{1}{2}(\varpi_{i,j} + \varpi_{j,i}) \tag{7}$$

$$\vec{\varpi} = \frac{1}{2}\vec{\nabla}\times\vec{U} \tag{8}$$

where $G = C_{55}$ is the shear modulus of elasticity, $\vec{U}$ is the displacement vector, l_0 is a material length scale parameter and ϖ is the rotation vector.

In EBBT displacement fields are expressed as [12]:

$$\begin{aligned} U(x,z,t) &= u(x,t) - z\frac{\partial w(x,t)}{\partial x} \\ W(x,z,t) &= w(x,t) \end{aligned} \tag{9}$$

and for TBT [13]:

$$\begin{aligned} U(x,t) &= u(x,t) + z\psi(x,t) \\ W(x,t) &= w(x,t) \end{aligned} \tag{10}$$

where $(\tilde{U},\tilde{W})$ are the axial and transverse displacements and ψ denotes the rotation of the cross-sectional area of the beam.

For EBBT Eqs. (6) and (7) are obtained as:

$$\begin{aligned}
&\chi_{yx} = \chi_{xy} = \frac{-1}{2}\left(\frac{\partial^2 w}{\partial x^2}\right)\\
&\chi_{xx} = \chi_{yy} = \chi_{zz} = \chi_{xz} = \chi_{yz} = 0\\
&m_{yx} = m_{xy} = 2C_{55}l_o{}^2\chi_{xy} = -C_{55}l_o{}^2\left(\frac{\partial^2 w}{\partial x^2}\right)\\
&m_{xx} = m_{yy} = m_{zz} = m_{xz} = m_{yz} = 0\\
&\varepsilon_{xx} = \frac{\partial U}{\partial x} = \frac{\partial u}{\partial x} - z\,\frac{\partial^2 w}{\partial x^2}\\
&\gamma_{xz} = \frac{\partial U}{\partial z} + \frac{\partial W}{\partial x} = 0
\end{aligned} \tag{11}$$

and for TBT Eqs. (6) and (7) are obtained as:

$$\begin{aligned}
&\chi_{yx} = \chi_{xy} = \frac{1}{4}\left(\frac{\partial \psi}{\partial x} - \frac{\partial^2 w}{\partial x^2}\right)\\
&\chi_{xx} = \chi_{yy} = \chi_{zz} = \chi_{xz} = \chi_{yz} = 0\\
&m_{yx} = m_{xy} = 2C_{55}l_0{}^2\chi_{xy} = \frac{1}{2}C_{55}l_0{}^2\left(\frac{\partial \psi}{\partial x} - \frac{\partial^2 w}{\partial x^2}\right)\\
&m_{xx} = m_{yy} = m_{zz} = m_{xz} = m_{yz} = 0\\
&\varepsilon_{xx} = \frac{\partial U}{\partial x} = \frac{\partial u}{\partial x} + z\,\frac{\partial \psi}{\partial x}\\
&\gamma_{xz} = \left(\frac{\partial W}{\partial x} + \frac{\partial U}{\partial z}\right) = \frac{\partial w}{\partial x} + \psi
\end{aligned} \tag{12}$$

According to Eq. (1) $(1\to y, 2\to z, 3\to x)$, in EBBT $\left(\varepsilon_{zx}=0, \varepsilon_{xy}=0, \varepsilon_{yz}=0\right)$, stress–strain relation and electric displacement for piezoelectric materials is given as follows:

$$\begin{aligned}
&\sigma_{xx} = C_{33}\varepsilon_{xx} - e_{33}E_x\\
&D_x = e_{33}\varepsilon_{xx} + \in_{33} E_x
\end{aligned} \tag{13}$$

and for TBT $\left(\varepsilon_{zx}\neq 0, \varepsilon_{xy}=0, \varepsilon_{yz}=0\right)$:

$$\begin{aligned}
&\sigma_{xx} = C_{33}\varepsilon_{xx} - e_{33}E_x\\
&\sigma_{xz} = C_{44}\left(\psi + \frac{\partial w}{\partial x}\right)\\
&D_x = e_{33}\varepsilon_{xx} + \in_{33} E_x
\end{aligned} \tag{14}$$

By substituting Eqs. (5), (11) and (13) into Eq. (4), the strain energy of micro-tube for EBBT can be obtained as:

$$U = \frac{1}{2}\int_V \left(\sigma_{xx}\varepsilon_{xx} + 2m_{xy}\chi_{xy} - D_x E_x\right)dV$$
$$= \frac{1}{2}\int_0^L \left(N_{xx}\left(\frac{\partial u}{\partial x}\right) - M_{xx}\left(\frac{\partial^2 w}{\partial x^2}\right) - P_{xy}\left(\frac{\partial^2 w}{\partial x^2}\right) + D_x\frac{\partial \phi}{\partial x}\right)dx \tag{15}$$

and by substituting Eqs. (5), (12) and (14) into Eq. (4), the strain energy of micro-tube for TBT can be obtained as:

$$U = \frac{1}{2}\int_V \left(\sigma_{xx}\varepsilon_{xx} + \sigma_{xz}\gamma_{xz} + 2m_{xy}\chi_{xy} - D_x E_x\right)dV$$
$$= \frac{1}{2}\int_0^L \left\{N_{xx}\left(\frac{\partial u}{\partial x}\right) + M_{xx}\left(\frac{\partial \psi}{\partial x}\right) + Q_{xz}\left(\psi + \frac{\partial w}{\partial x}\right) + \frac{1}{2}P_{xy}\left(\frac{\partial \psi}{\partial x} - \frac{\partial^2 w}{\partial x^2}\right) + D_x\frac{\partial \phi}{\partial x}\right\}dx \tag{16}$$

The stress resultants introduced in Eqs. (15) and (16) are defined as:

$$N_{xx} = \int_{A_t}\sigma_{xx}dA_t, \qquad M_{xx} = \int_{A_t}\sigma_{xx}z^2 dA_t, \qquad Q_{xz} = \int_{A_t}\sigma_{xz}dA_t, \qquad P_{xy} = \int_{A_t} m_{xy}dA_t \tag{17}$$

and kinetic energy of the micro-tube is:

$$K_{tube} = \frac{1}{2}\rho_t\int_0^L\int_{A_t}\left\{\left(\frac{\partial U(x,t)}{\partial t}\right)^2 + \left(\frac{\partial W(x,t)}{\partial t}\right)^2\right\}dA_t\,dx \tag{18}$$

where ρ_t denote the density of micro-tube.

4 FLUID STRUCTURE INTERACTION

4.1 Navier-Stokes equations

The Navier–Stokes equations describe the motion of viscous fluid substances. It may be used to model the water flow in a pipe and air flow around a wing. The Navier–Stokes equations in their full and simplified forms help with the design of aircraft and cars, the study of blood flow and many other things [14].

To evaluate the effect fluid flow on composite micro-tube, Navier–Stokes equation can be used as [15]:

$$\rho_f\frac{d\vec{V}}{dt} = -\nabla P + \mu_f\nabla^2\vec{V} \tag{19}$$

where ρ_f, P and μ_f fluid density, static pressure and fluid viscosity, respectively and d/dt can be defined as follows:

$$\frac{d}{dt} = \frac{\partial}{\partial t} + u_f\frac{\partial}{\partial x} \tag{20}$$

It is worth mentioning that the left hand of Navier-stokes equation present the kinetic energy of flow fluid. In this research, it's considered a Newtonian fluid can be passed through the micro-tube with constant velocity at the first and end of micro-tube. The fluid flow is assumed to be incompressible, viscous and irrotational. Velocity field vector ($\vec{V} = V_x, V_z$) for the fluid is the relative velocity including fluid and nanotube velocity. This vector can be expressed as [16]:

$$V_x = \frac{\partial U(x,t)}{\partial t} + u_f \cos(\theta)$$
$$V_z = \frac{\partial W(x,t)}{\partial t} - u_f \sin(\theta) \tag{21}$$

where $\theta = -\frac{\partial w}{\partial x}$ and u_f is the fluid velocity.

Using Eq. (21) and (19), it can be expanded in directions x, z for EBBT as follows:

$$\frac{\partial P}{\partial x} = -\rho_f \frac{\partial^2 u}{\partial t^2} + \rho_f z \frac{\partial^3 w}{\partial x \partial t^2} - \rho_f \left(\frac{du_f}{dt}\right)\cos(\theta) - \rho_f u_f \sin(\theta)\frac{\partial^2 w}{\partial x \partial t} - \rho_f u_f \frac{\partial^2 u}{\partial x \partial t} + \rho_f u_f z \frac{\partial^3 w}{\partial x^2 \partial t}$$
$$-\rho_f u_f{}^2 \sin(\theta)\frac{\partial^2 w}{\partial x^2} + \mu_f \frac{\partial^3 u}{\partial x^2 \partial t} - \mu_f z \frac{\partial^4 w}{\partial x^3 \partial t} - \mu_f u_f \cos(\theta)\left(\frac{\partial^2 w}{\partial x^2}\right)^2 + \mu_f u_f \sin(\theta)\frac{\partial^3 w}{\partial x^3} \tag{22}$$

$$\frac{\partial P}{\partial z} = -\rho_f \frac{\partial^2 w}{\partial t^2} + \rho_f \left(\frac{du_f}{dt}\right)\sin(\theta) - \rho_f u_f \cos(\theta)\frac{\partial^2 w}{\partial x \partial t} - \rho_f u_f \frac{\partial^2 w}{\partial x \partial t} - \rho_f u_f{}^2 \cos(\theta)\frac{\partial^2 w}{\partial x^2}$$
$$+\mu_f \frac{\partial^3 w}{\partial x^2 \partial t} + \mu_f u_f \sin(\theta)\left(\frac{\partial^2 w}{\partial x^2}\right)^2 + \mu_f u_f \cos(\theta)\frac{\partial^3 w}{\partial x^3} \tag{23}$$

and for TBT:

$$\frac{\partial P}{\partial x} = -\rho_f \frac{\partial^2 u}{\partial t^2} - \rho_f z \frac{\partial^2 \psi}{\partial t^2} - \rho_f \left(\frac{du_f}{dt}\right)\cos(\theta) - \rho_f u_f \sin(\theta)\frac{\partial^2 w}{\partial x \partial t} - \rho_f u_f \frac{\partial^2 u}{\partial x \partial t} - \rho_f u_f z \frac{\partial^2 \psi}{\partial x \partial t}$$
$$-\rho_f u_f{}^2 \sin(\theta)\frac{\partial^2 w}{\partial x^2} + \mu_f \frac{\partial^3 u}{\partial x^2 \partial t} + \mu_f z \frac{\partial^3 \psi}{\partial x^2 \partial t} - \mu_f u_f \cos(\theta)\left(\frac{\partial^2 w}{\partial x^2}\right)^2 + \mu_f u_f \sin(\theta)\frac{\partial^3 w}{\partial x^3} \tag{24}$$

$$\frac{\partial P}{\partial z} = -\rho_f \frac{\partial^2 w}{\partial t^2} + \rho_f \left(\frac{d}{dt}u_f(t)\right)\sin(\theta) - \rho_f u_f \cos(\theta)\frac{\partial^2 w}{\partial x \partial t} - \rho_f u_f \frac{\partial^2 w}{\partial x \partial t} - \rho_f u_f{}^2 \cos(\theta)\frac{\partial^2 w}{\partial x^2}$$
$$+\mu_f \frac{\partial^3 w}{\partial x^2 \partial t} + \mu_f u_f \sin(\theta)\left(\frac{\partial^2 w}{\partial x^2}\right)^2 + \mu_f u_f \cos(\theta)\frac{\partial^3 w}{\partial x^3} \tag{25}$$

The virtual work down by fluid can be calculated as follows:

$$\Omega_{Fluid} = \int_0^L \int_{A_f} \left[\frac{\partial P}{\partial x}(\delta U) + \frac{\partial P}{\partial z}(\delta W)\right] dA_f\, dx \tag{26}$$

4.2 Knudsen number

Knudsen number is a dimensionless parameter defined as the ratio of the mean-free-path of the molecules to a characteristic length scale which is used for identifying the various flow regimes. For micro and nanotubes, the radius of the tube is assumed as the characteristic length scale.

According to the Knudsen number the classification of the various flow regimes is given as: continuum flow regime $(Kn \prec 10^{-2})$, slip flow regime $(10^{-2} \prec Kn \prec 10^{-1})$, transition flow regime $(10^{-1} \prec Kn \prec 10)$, free molecular flow regime $(Kn \succ 10)$ [17]. For BNNT conveying fluid, Kn may be larger than 10^{-2}. Therefore, the assumption of no-slip boundary conditions is no longer credible, and a modified model must be used.

So $V_{avg,slip}$ is replaced by $VCF \times V_{avg,(no-slip)}$ in the basic equations, that VCF is determined as follows[18]:

$$VCF \equiv \frac{V_{avg,slip}}{V_{avg,(no-slip)}} = (1+aKn)\left[1+4\left(\frac{2-\sigma_v}{\sigma_v}\right)\left(\frac{Kn}{1+Kn}\right)\right] \tag{27}$$

where σ_v is tangential momentum accommodation coefficient. For most practical applications σ_v is chosen to be 0.7 and a can be expressed as the following relation:

$$a = a_0 \frac{2}{\pi}\left[\tan^{-1}\left(a_1 Kn^B\right)\right] \tag{28}$$

In which, $a_1 = 4$ and $B = 0.04$, are some experimental parameters. The coefficient a_0 is formulated as:

$$\lim_{Kn\to\infty} a = a_0 = \frac{64}{3\pi\left(1-\frac{4}{b}\right)} \tag{29}$$

where $b = -1$.

5 VISCO-PASTERNAK FOUNDATION

Based on the Winkler and Visco-Pasternak foundations, the effects of surrounding elastic medium on the nanotubes are considered as follows [19]:

$$F_{Elsatic} = K_w w - K_G \frac{\partial^2 w}{\partial x^2} \tag{30}$$

where $F_{Elsatic}$ is the external forces applied on micro-tube. The external work due to surrounding elastic and the dissipation energy by dampers acting on micro-tube are written as:

$$\begin{aligned} W_{Elastic} &= \frac{1}{2}\int_0^L F_{Elsatic} w\, dx \\ W_{damping} &= \frac{1}{2}\int_0^L C_d \left(\frac{\partial w}{\partial t}\right)^2 dx \end{aligned} \tag{31}$$

where k_w , k_G and C_d is Winkler and Pasternak modulus besides damping coefficient.

6 MAXWELL'S RELATIONS

In this section, the virtual work (effects) of 2D magnetic field (longitudinal and transversal) on microtube due to CNT fibres has been studied by Maxwell's relations. Denoting *J* as current density, *h* as distributing vector of the magnetic field, *e* as strength vectors of the electric field and *f* as the Lorentz force, the Maxwell relations according to [20] is given as:

$$
\begin{aligned}
&J = \nabla \times h \\
&\nabla \times e = -\eta \frac{\partial h}{\partial t} \\
&\nabla \cdot h = 0 \\
&e = -\eta \left(\frac{\partial h}{\partial t} \times H \right) \\
&h = \nabla \times \left(U \times H \right) \\
&f = f_x \hat{i} + f_x \hat{j} + f_x \hat{k} = \eta \left(J \times h \right)
\end{aligned}
\tag{32}
$$

where the Hamilton arithmetic operator is $\nabla = \frac{\partial}{\partial x}\hat{i} + \frac{\partial}{\partial z}\hat{k}$ and η is the magnetic permeability. The displacement vector for EBBT is $\overline{U} = \left[u(x,t) - z \frac{\partial w(x,t)}{\partial x} \right] \hat{i} + w(x,t)\hat{j}$ and for TBT is $\vec{U} = \left[u(x,t) + z\psi(x,t) \right] \hat{i} + w(x,t)\hat{j}$. By considering 2D magnetic field as a vector $\overrightarrow{H} = H_x \hat{i} + H_z \hat{k}$ acting on the CNT fibers, the components of Lorentz force induced by the 2D magnetic field for EBBT is:

$$
\begin{aligned}
&f_x = \eta H_z^2 \left(\frac{\partial^2 u}{\partial x^2} - z \frac{\partial^3 w}{\partial x^3} \right) - \eta H_x H_z \left(\frac{\partial^2 w}{\partial x^2} \right) \\
&f_y = 0 \\
&f_z = -\eta H_x H_z \left(\frac{\partial^2 u}{\partial x^2} - z \frac{\partial^3 w}{\partial x^3} \right) + \eta H_x^2 \left(\frac{\partial^2 w}{\partial x^2} \right)
\end{aligned}
\tag{33}
$$

and for TBT is:

$$
\begin{aligned}
&f_x = \eta H_z^2 \left(\frac{\partial^2 u}{\partial x^2} + z \frac{\partial^2 \psi}{\partial x^2} \right) - \eta H_x H_z \left(\frac{\partial^2 w}{\partial x^2} \right) \\
&f_y = 0 \\
&f_z = -\eta H_x H_z \left(\frac{\partial^2 u}{\partial x^2} + z \frac{\partial^2 \psi}{\partial x^2} \right) + \eta H_x^2 \left(\frac{\partial^2 w}{\partial x^2} \right)
\end{aligned}
\tag{34}
$$

So the virtual work due to 2D magnetic field is written as:

$$
\delta \Omega_{magnetic} = \int_0^L \int_{A_t} \left(f_x \times \delta U + f_z \times \delta W \right) dA_t dx \tag{35}
$$

7 MOTION EQUATIONS

Using Hamilton's principle the variational form of the equations of motion can be written as:

$$
\begin{aligned}
\int_{t_0}^{t_1} \delta \Pi dt &= \delta \int_{t_1}^{t_2} \left[K - (U - \Omega) \right] dt = 0 \\
&= \int_{t_0}^{t_1} \left(\delta U - \delta K_{tube} - \delta \Omega_{elastic} - \delta \Omega_{magnetic} - \Omega_{Fluid} \right) dt = 0
\end{aligned}
\tag{36}
$$

For simplification the dimensionless parameters are defined as:

$$X=\frac{x}{L} \qquad (U,W)=\frac{(u,w)}{r} \qquad T=\frac{t}{L}\sqrt{\frac{C_{33}^{m}}{\rho_t}} \qquad \lambda=\frac{L}{r}$$
$$\bar{\phi}=\frac{\phi e_{33}}{LC_{33}^{m}} \qquad \gamma=\frac{\in_{33} C_{33}^{m}}{h_{11}^{2}} \qquad (\overline{C_{33}},\overline{C_{44}})=\frac{(C_{33},C_{44})}{C_{33}^{m}} \qquad \overline{C_d}=\frac{C_d L}{\sqrt{C_{33}^{m}\rho_t}A_t}$$
$$\bar{A}=\frac{A_f}{A_t} \qquad \overline{\rho_f}=\frac{\rho_f}{\rho_m} \qquad \overline{\rho_t}=\frac{\rho_t}{\rho_m} \qquad \overline{u_f}=\sqrt{\frac{\rho_f}{C_{33}^{m}}}u_f \tag{37}$$
$$\bar{\mu}_f=\frac{\mu_f}{L\sqrt{C_{33}^{m}\rho_f}} \qquad \left(\overline{I_t},\overline{I_f}\right)=\frac{(I_f,I_t)}{A_t r^2} \qquad \overline{K_w}=\frac{K_w L^2}{A_t C_{33}^{m}} \qquad \overline{K_G}=\frac{K_G}{A_t C_{33}^{m}}$$
$$(\overline{H_x},\overline{H_y},\overline{H_z})=\lambda\sqrt{\frac{\eta}{C_{33}^{m}}}(H_x,H_y,H_z)$$

By setting the coefficients of $\delta u,\delta w,\delta\psi$ and $\delta\varphi$ equal to zero the motion equation can be obtained. It's also assumed that θ is small so cosθ≈ 1 and sinθ≈ θ. the equation of motion for EBBT are obtained as follows:

$$\delta u:\overline{\rho_t}\frac{\partial^2 U}{\partial T^2}+\overline{\rho_f}\,\overline{A}\frac{\partial^2 U}{\partial T^2}+\frac{1}{\lambda^2}\overline{H_x}\,\overline{H_z}\frac{\partial^2 W}{\partial X^2}-\sqrt{\overline{\rho_f}}\,\overline{A}\,\overline{\mu_f}\frac{\partial^3 U}{\partial X^2\partial T}-\frac{1}{\lambda^2}\overline{H_z}^{2}\frac{\partial^2 U}{\partial X^2}-\lambda\frac{\partial^2\bar{\phi}}{\partial X^2}$$
$$+2\sqrt{\overline{\rho_f}}\,\overline{A}\lambda\frac{d\overline{u_f}}{dT}-\overline{C_{33}}\frac{\partial^2 U}{\partial X^2} \tag{38}$$

$$\delta w:\overline{\rho_t}\frac{\partial^2 W}{\partial T^2}+\overline{K_w}W-\overline{K_G}\frac{\partial^2 W}{\partial X^2}+\overline{C_d}\frac{\partial W}{\partial T}+\overline{A}\,\overline{u_f}^{2}\frac{\partial^2 W}{\partial X^2}+\overline{\rho_f}\,\overline{A}\frac{\partial^2 W}{\partial T^2}+\frac{1}{\lambda^2}\overline{I_t}\,\overline{H_z}^{2}\frac{\partial^4 W}{\partial X^4}+\frac{1}{\lambda^2}\overline{\mu_f}\sqrt{\overline{\rho_f}}\,\overline{I_f}\frac{\partial^5 W}{\partial X^4\partial T}$$
$$-\overline{A}\,\overline{\mu_f}\sqrt{\overline{\rho_f}}\frac{\partial^3 W}{\partial X^2\partial T}+\frac{1}{\lambda^2}\overline{H_x}\,\overline{H_z}\frac{\partial^2 U}{\partial X^2}-\frac{1}{\lambda^2}\overline{\rho_f}\,\overline{I_f}\left(\frac{\partial^4 W}{\partial X^2\partial T^2}\right)+\frac{1}{\lambda^2}\overline{C_{33}}\,\overline{I_t}\frac{\partial^4 W}{\partial X^4}-\overline{A}\,\overline{\mu_f}\,\overline{u_f}\frac{\partial^3 W}{\partial X^3} \tag{39}$$
$$+2\sqrt{\overline{\rho_f}}\,\overline{A}\left(\frac{\partial^2 W}{\partial X\,\partial T}\right)\overline{u_f}+2\sqrt{\overline{\rho_f}}\,\overline{A}\left(\frac{d\overline{u_f}}{dT}\right)\frac{\partial W}{\partial X}-\frac{1}{\lambda^2}\overline{\rho_t}\,\overline{I_t}\frac{\partial^4 W}{\partial X^2\partial T^2}-\frac{1}{\lambda^2}\overline{H_x}^{2}\frac{\partial^2 W}{\partial X^2}+\overline{C_{44}}\,\overline{l_0}^{2}\left(\frac{\partial^4 W}{\partial X^4}\right)$$

$$\delta\phi:-\frac{\partial^2 U}{\partial x^2}+\gamma\lambda\frac{\partial^2\bar{\phi}}{\partial x^2} \tag{40}$$

and for TBT:

$$\delta u:\overline{\rho_t}\frac{\partial^2 U}{\partial T^2}+\overline{\rho_f}\,\overline{A}\frac{\partial^2 U}{\partial T^2}+\frac{1}{\lambda^2}\overline{H_x}\,\overline{H_z}\frac{\partial^2 W}{\partial X^2}-\sqrt{\overline{\rho_f}}\,\overline{A}\,\overline{\mu_f}\frac{\partial^3 U}{\partial X^2\partial T}-\frac{1}{\lambda^2}\overline{H_z}^{2}\frac{\partial^2 U}{\partial X^2}-\lambda\frac{\partial^2\bar{\phi}}{\partial X^2}$$
$$+2\sqrt{\overline{\rho_f}}\,\overline{A}\lambda\frac{d\overline{u_f}}{dT}-\overline{C_{33}}\frac{\partial^2 U}{\partial X^2} \tag{41}$$

$$\delta w:\overline{K_w}W-\overline{K_G}\frac{\partial^2 W}{\partial X^2}+\frac{1}{\lambda^2}\overline{H_x}\,\overline{H_z}\frac{\partial^2 U}{\partial X^2}-\overline{A}\,\overline{\mu_f}\sqrt{\overline{\rho_f}}\frac{\partial^3 W}{\partial X^2\partial T}-K_s\overline{C_{44}}\lambda\frac{\partial\psi}{\partial X}+\overline{C_d}\frac{\partial W}{\partial T}-\overline{A}\,\overline{\mu_f}\,\overline{u_f}\frac{\partial^3 W}{\partial X^3}$$
$$+2\sqrt{\overline{\rho_f}}\,\overline{A}\left(\frac{d\overline{u_f}}{dT}\right)\frac{\partial W}{\partial X}+2\sqrt{\overline{\rho_f}}\,\overline{A}\left(\frac{\partial^2 W}{\partial X\,\partial T}\right)\overline{u_f}+\overline{A}\,\overline{u_f}^{2}\frac{\partial^2 W}{\partial X^2}+\overline{\rho_t}\frac{\partial^2 W}{\partial T^2}+\overline{\rho_f}\,\overline{A}\frac{\partial^2 W}{\partial T^2}-\frac{1}{\lambda^2}\overline{H_x}^{2}\frac{\partial^2 W}{\partial X^2} \tag{42}$$
$$-K_s\overline{C_{44}}\frac{\partial^2 W}{\partial X^2}-\frac{1}{4}\lambda\overline{C_{44}}\,\overline{l_0}^{2}\left(\frac{\partial^3\psi}{\partial X^3}\right)+\frac{1}{4}\overline{C_{44}}\,\overline{l_0}^{2}\left(\frac{\partial^4 w}{\partial X^4}\right)$$

$$\delta\psi : -\overline{\mu_f}\sqrt{\overline{\rho_f}}\,\overline{I_f}\frac{\partial^3\psi}{\partial X^2\partial T} - \frac{1}{\lambda^2}\overline{I_t}\,\overline{H_z}^2\frac{\partial^2\psi}{\partial X^2} + \lambda^2 K_s\overline{C_{44}}\psi + \overline{\rho_t}\,\overline{I_t}\frac{\partial^2\psi}{\partial T^2} + \overline{\rho_f}\,\overline{I_f}\frac{\partial^2\psi}{\partial T^2} + \lambda K_s\overline{C_{44}}\frac{\partial W}{\partial X}$$
$$-\overline{C_{33}}\,\overline{I_t}\frac{\partial^2\psi}{\partial X^2} - \frac{1}{4}\lambda^2\overline{C_{44}}\,\overline{l_0}^2\left(\frac{\partial^2\psi}{\partial X^2}\right) + \frac{1}{4}\lambda\overline{C_{44}}\,\overline{l_0}^2\left(\frac{\partial^3 W}{\partial X^3}\right) \tag{43}$$

$$\delta\phi : -\frac{\partial^2 U}{\partial x^2} + \gamma\lambda\frac{\partial^2\overline{\phi}}{\partial x^2} \tag{44}$$

8 SOLUTION METHOD

The wave propagation solution of Eqs. (38) to (44) for simply supported boundary condition can be expressed as follows:

$$\begin{aligned} U &= U_0 e^{i\,\mathrm{kX}+\omega T} \\ W &= W_0\, e^{i\,\mathrm{kX}+\omega T} \\ \psi &= \psi_0\, e^{i\,\mathrm{kX}+\omega T} \\ \phi &= \phi_0\, e^{i\,\mathrm{kX}+\omega T} \end{aligned} \tag{45}$$

where U_0, ψ_0, W_0, ϕ_0 are the wave amplitude, $k\,(L.K)$ is the dimensionless wave number and ω is the dimensionless complex frequency of wave motion. By substituting Eq. (49) into Eqs. (38) to (44) for EBBT:

$$\begin{bmatrix} M_{11} & M_{12} & M_{13} \\ M_{21} & M_{11} & 0 \\ M_{31} & 0 & M_{33} \end{bmatrix}\begin{bmatrix} U_0 \\ W_0 \\ \phi_0 \end{bmatrix} = \begin{Bmatrix} 0 \\ 0 \\ 0 \end{Bmatrix} \tag{46}$$

and for TBT:

$$\begin{bmatrix} M_{11} & M_{12} & 0 & M_{14} \\ M_{21} & M_{22} & M_{23} & 0 \\ 0 & M_{32} & M_{33} & 0 \\ M_{41} & 0 & 0 & M_{44} \end{bmatrix}\begin{bmatrix} U_0 \\ W_0 \\ \psi_0 \\ \phi_0 \end{bmatrix} = \begin{Bmatrix} 0 \\ 0 \\ 0 \\ 0 \end{Bmatrix} \tag{47}$$

where M_{ij} for EBBT are given by:

$$\begin{aligned} M_{11} &= \left(\overline{A}\,\lambda^2\overline{\rho_f} + \lambda^2\overline{\rho_t}\right)\omega^2 + \left(\overline{A}\,\overline{\mu_f}\sqrt{\overline{\rho_f}}\,k^2\lambda^2\right)\omega + \overline{C_{33}}k^2\lambda^2 + \overline{H_z}^2 k^2 \\ M_{12} &= -\overline{H_x}\,\overline{H_z}\,k^2, \qquad M_{13} = k^2\lambda^3, \qquad M_{21} = -\overline{H_x}\,\overline{H_z}\,k^2\lambda^2 \\ M_{22} &= \left(\overline{I_f}\,k^2\lambda^2\overline{\rho_f} + \overline{I_t}\,k^2\lambda^2\overline{\rho_t} + \lambda^4\overline{\rho_t} + \overline{A}\,\lambda^4\overline{\rho_f}\right)\omega^2 \\ &\quad + \left(\overline{C_d}\,\lambda^4 + \overline{A}\,\overline{\mu_f}\sqrt{\overline{\rho_f}}\,k^2\lambda^4 + \overline{\mu_f}\sqrt{\overline{\rho_f}}\,\overline{I_f}\,k^4\lambda^2 + 2i\,\overline{A}\,k\sqrt{\overline{\rho_f}}VCF\overline{u_f}\,\lambda^4\right)\omega \\ &\quad + \overline{I_t}\,\overline{H_z}^2 k^4 + \overline{H_x}^2 k^2\lambda^2 + \overline{K_g}\,k^2\lambda^4 - \overline{A}VCF^2\overline{u_f}^2 k^2\lambda^4 + i\,\overline{A}\,\overline{\mu_f}VCF\,\overline{u_f}\,k^3\lambda^4 \\ &\quad + \overline{K_w}\,\lambda^4 + \overline{C_{33}}\,\overline{I_t}\,k^4\lambda^2 + \overline{C_{44}}\,\overline{I_0}k^4\lambda^4 \\ M_{31} &= k^2, \qquad M_{33} = -k^2\gamma\lambda \end{aligned} \tag{48}$$

where M_{ij} for TBT are given by:

$$
\begin{aligned}
M_{11} &= \left(\overline{A}\lambda^2\overline{\rho_f} + \lambda^2\overline{\rho_t}\right)\omega^2 + \left(\overline{A}k^2\lambda^2\overline{\mu_f}\right)\omega + \overline{C_{33}}k^2\lambda^2 + \overline{H_z}^2k^2 \\
M_{22} &= \left(\overline{A}\lambda^2\overline{\rho_f} + \lambda^2\overline{\rho_t}\right)\omega^2 + \left(2i\overline{A}k\sqrt{\overline{\rho_f}}VCF\,\overline{u_f}\lambda^2 + \overline{A}k^2\lambda^2\overline{\mu_f} + \overline{C_d}\lambda^2\right)\omega \\
&\quad + \overline{K_g}k^2\lambda^2 - \overline{A}VCF^2\overline{u_f}^2k^2\lambda^2 + K_s\overline{C_{44}}k^2\lambda^2 + i\overline{A}\,\overline{\mu_f}VCF\,\overline{u_f}k^3\lambda^2 + \overline{H_x}^2k^2 \\
M_{33} &= \left(\overline{I_f}\lambda^2\overline{\rho_f} + \overline{I_t}\lambda^2\overline{\rho_t}\right)\omega^2 + \left(\overline{\mu_f}\sqrt{\overline{\rho_f}}\,\overline{I_f}k^2\lambda^2\right)\omega + \overline{C_{33}}\,\overline{I_t}k^2\lambda^2 + \overline{C_{44}}K_s\lambda^4 + \overline{H_z}^2\overline{I_t}k^2 + \frac{1}{4}\overline{C_{44}}\,\overline{l_0}^2k^4\lambda^2 \\
M_{12} &= -\overline{H_x}\,\overline{H_z}k^2, \qquad M_{14} = k^2\lambda^3, \qquad M_{21} = -\overline{H_x}\,\overline{H_z}k^2 \\
M_{23} &= -iK_s\overline{C_{44}}k\lambda^3 + \frac{1}{4}i\overline{C_{44}}\,\overline{l_0}^2k^3\lambda^3, \qquad M_{32} = iK_s\overline{C_{44}}k\lambda^3 - \frac{1}{4}i\overline{C_{44}}\,\overline{l_0}^2k^3\lambda^3 \\
M_{41} &= k^2, \qquad M_{44} = -k^2\gamma\lambda
\end{aligned}
\tag{49}
$$

In order to obtain a non-trivial solution, it is necessary to set the determinant of the coefficient matrix in Eqs. (46) and (47) equal to zero which yields the algebraic equation. This equation can be solved through a direct iterative process to evaluate frequency of the micro-tube and consequently phase velocity from $c = \omega/k$.

9 NUMERICAL RESULTS AND DISCUSSION

In this section the result of wave propagation analysis in polymeric smart nanocomposite micro-tubes subjected to electro-magneto-mechanical fields is studied. The matrix of composite has been mad of PVDF and reinforced by SWCNT while a Newtonian fluid passes through it with constant velocity. Visco-Pasternak model was also selected to simulate the surrounded elastic medium. The results presented here are based on Table 1., that used for geometry and material properties of PVDF and CNT [21]. It's assumed that the water passes through the micro-composite with: $\rho_f = 1000\left(Kg/m^3\right)$, $\mu = 0.653\times10^{-3}\left(N.s/m^2\right)$, $Kn = 0.02$ and $\overline{u_f} = 0.05$.

Table 1
Material properties of PVDF and CNT [21].

	ρ	C_{33}	C_{44}	e_{33}	$\in_{33}/\in_0$
CNT	$1400\left(Kg/m^3\right)$	$1444.2(Gpa)$	$1191.5(Gpa)$	$0\left(C/m^2\right)$	0.1
PVDF	$1780\left(Kg/m^3\right)$	$238.24(Gpa)$	$215(Gpa)$	$-0.13\left(C/m^2\right)$	12.5
$\in_0 = 8.854185\times10^{-12}\left(F/m\right)$					

The numerical values of other parameters have been considered as follows:

$$k_s = 0.6, \lambda = 80, \overline{H}_x = 5, \overline{H}_y = \overline{H}_z = 0, \rho_r = 0.3, \overline{K}_w = 0.2, \overline{K}_G = 0.01, \overline{C}_d = 1, h = 0.34(\mu m), r_i = 3.4(\mu m)$$

In this section, effects of dimensionless parameters such as Winkler and Visco-Pasternak modules, Knudsen number (Kn), cutoff and escape frequency, fluid viscosity and length scale on the dimensionless phase velocity and fluid velocity of two simply supported composite cylinder are shown in Figs. 2 to 9.

Figs. 2(a) and 2(b) shows the effect of viscoelastic medium on dimensionless phase velocity versus dimensionless wave number for EBBT and TBT. Three type of elastic medium have been considered in this research including: Winkler, Pasternak and Visco-Pasternak foundation. Visco-Pasternak foundation introduces the damping coefficient cd in spite of normal K_w and shear modulus K_g . As can be seen from the Figs. 2(a) and 2(b), normal and shear modulus in Winkler and Pasternak models play a positive role to stability of system while damping effect lead to instability. On the other hand, in large dimensionless wave number, the difference among three models becomes more visible.

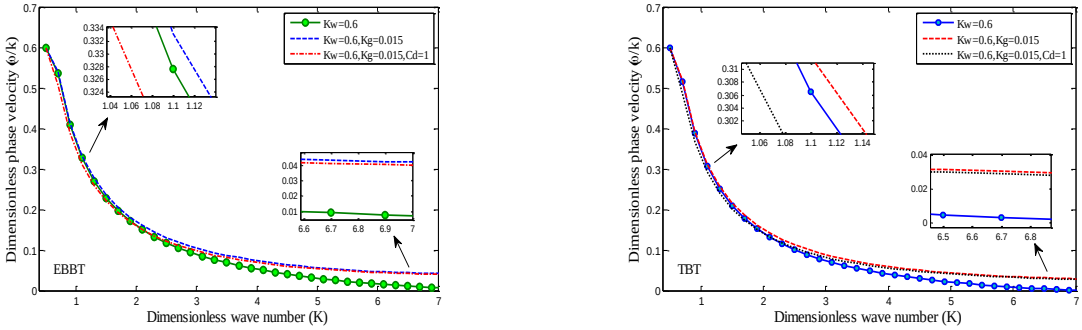

(a) (b)

Fig.2
a) Effect of viscoelastic medium on dimensionless phase velocity versus dimensionless wave number for EBBT. b) Effect of viscoelastic medium on dimensionless phase velocity versus dimensionless wave number for TBT.

To show the effect of fluid density and viscosity on the dimensionless phase velocity, Fig. 3 was drawn for TBT. Since it's not possible to investigate the viscosity in a special numerical rang, we considered three Newtonian fluid with specific feature that used in many fluid structure interaction such as Aston, Water and Blood (Blood is considered Newtonian fluid in some conditions). It's clear from the figure that the changes in the results are negligible so that it can be ignored.

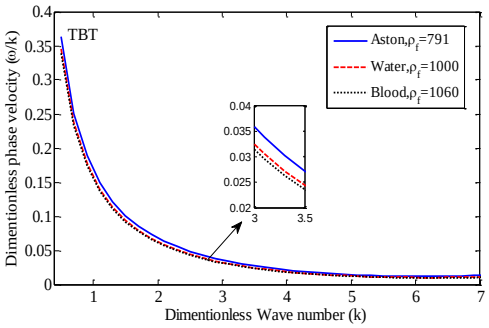

Fig.3
Effect of fluid density and viscosity on the dimensionless phase velocity for TBT.

The characteristics of elastic wave propagation for a given wave number investigate in two different waves, propagating in two opposite directions of upstream and downstream. The corresponding wave frequencies are called upstream and downstream frequencies [22]. According to Ref. [5] the numerical results demonstrate that these frequencies have different values when there is a fluid flowing through a tube with an infinite length. These wave frequencies are the same when there is either no flow or the flow is still [23]. Also in Ref. [5], the difference between upstream and downstream have been clearly stated.

Figs. 4(a) and 4(b) shows variation of dimensionless phase velocity versus dimensionless wave number for EBBT and TBT in different length scale parameters. As can be seen from the figure with increasing length scale parameters in modified couple stress theory the dimensionless phase velocity shift up. Comparison between the Figs. 4(a) and 4(b) shows that the dimensionless phase velocity in EBBT is more than TBT. For both beam models, two phase velocity curves of upstream and downstream waves join at higher wave numbers that indicate the fluid flow has no effect in the wave propagation of the higher wave numbers. The dimensionless phase velocity decreases and become zero at dimensionless wave number, indicating the critical fluid velocity is reached and the tube losses its stability.

Figs. 5(a) and 5(b) shows the variation of dimensionless phase velocity versus dimensionless wave number for EBBT and TBT in different volume fraction of CNT. It is evident when the volume fraction of fibers increases the composite becomes stronger so the dimensionless phase velocity grows to higher values.

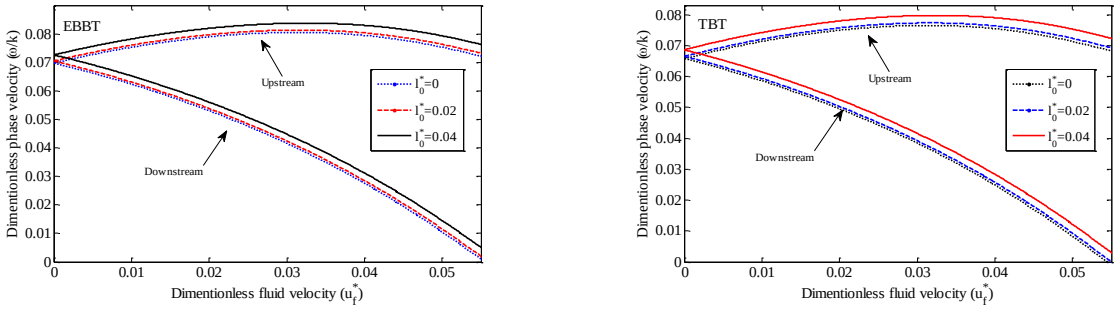

Fig.4
a) Variation of dimensionless phase velocity versus dimensionless wave number for EBBT in different length scale parameters.
b) Variation of dimensionless phase velocity versus dimensionless wave number for TBT in different length scale parameters.

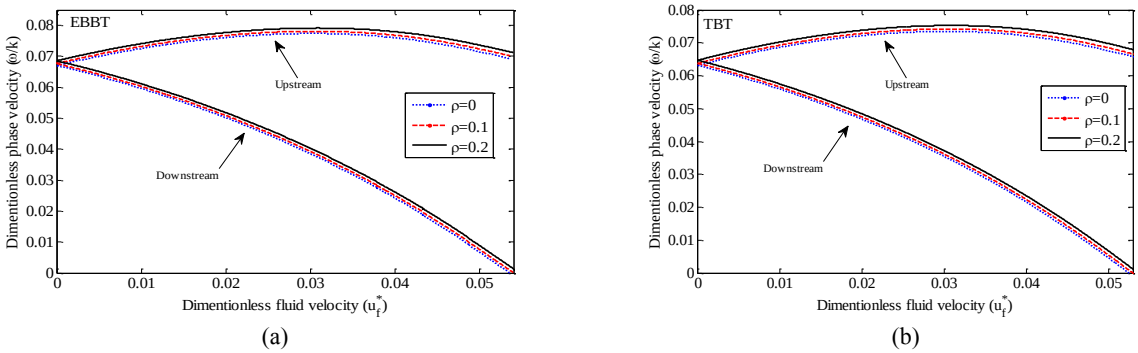

Fig.5
a) Variation of dimensionless phase velocity versus dimensionless wave number for EBBT in different volume fraction of CNT.
b) Variation of dimensionless phase velocity versus dimensionless wave number for TBT in different volume fraction of CNT.

In physics, a cutoff frequency is a boundary in a system's frequency response at which energy flowing through the system begins to be reduced rather than passing through. In the case of a waveguide, the cutoff frequencies correspond to the lower and upper cutoff wavelengths. The cutoff frequency of a waveguide is the lowest frequency for which a mode will propagate in it.

Cutoff frequency is obtained by setting the longitudinal wave number equal to zero and solving for the frequency. Any exciting frequency lower than the cutoff frequency will attenuate, rather than propagate.

Fig. 6 displays the variation of dimensionless cutoff frequency in a limited interval of dimensionless fluid velocity. It's found from the figure that the cutoff frequency decreases linearly and sharply with increasing the dimensionless fluid velocity but the slop of changes in EBBT is lower than TBT, while the first value of cutoff frequency in $u_f = 0$ is the same for both theories.

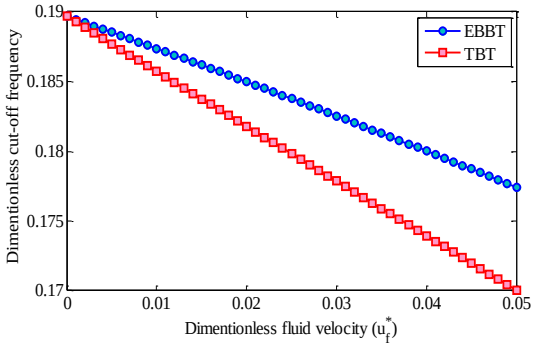

Fig.6
Variation of dimensionless cutoff frequency versus dimensionless fluid velocity.

Fig. 7 illustrates the variation of dimensionless escape frequency (when $k \to \infty$) in a limited interval of dimensionless fluid velocity. Finding shows that the escape frequency decreases with increasing dimensionless fluid velocity for both EBBT and TBT. Unlike cutoff frequency, the first value of escape frequency is not equal for two beam theories and with increasing dimensionless fluid velocity, two curves get close to each other.

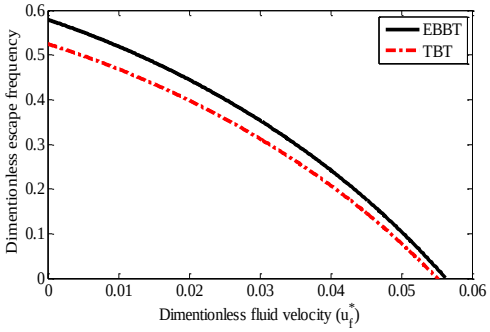

Fig.7
Variation of dimensionless escape frequency versus dimensionless fluid velocity.

Effect of Knudsen number on dimensionless phase velocity of composite micro-tube is illustrated in Figs. 8(a) and 8(b). Knudsen number is defined based on the type of flow regimes and in this research the slip flow regime has been considered. As shown in these figures, continuum fluid ($K_n = 0$) predicts the highest dimensionless phase velocity where by increasing Knudsen number the dimensionless phase velocity reduces. The result of both EBBT and TBT are the same but the values of Fig. 8(a) are larger than Fig. 8(b).

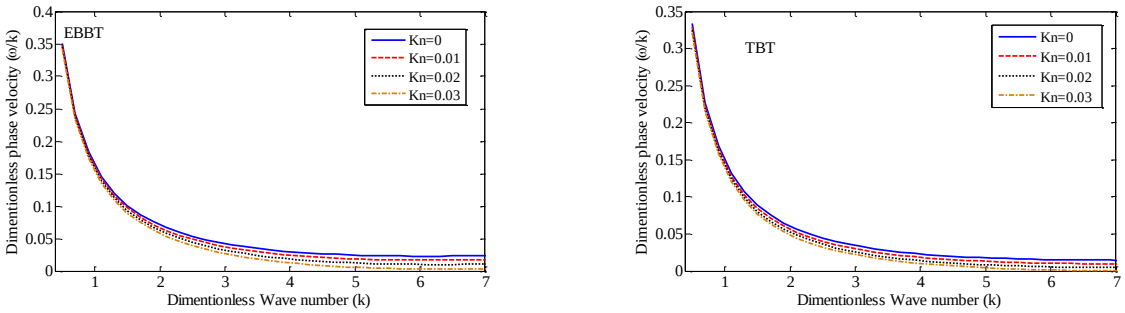

Fig.8
a) Effect of Knudsen number on dimensionless phase velocity for EBBT. b) Effect of Knudsen number on dimensionless phase velocity for TBT.

As mentioned in this work 2D magnetic field has been applied on nanocomposite cylindrical micro-tube reinforced by CNTs in x and z directions. Figs. 9(a) to 9(d) show the effect of magnetic field on dimensionless phase velocity. In this regard four figures have been plotted in which Fig. 9(a) and 9(c) show the effect of H_x on the phase velocity for EBBT and TBT and Fig. 9(b) and 9(d) have been drawn for the simultaneous effect of H_x and H_z. Results clearly reveal that the *x*-direction magnetic field is more significant than *z*-direction on wave propagation because the Lorentz force created by H_x applied in *z* direction but it generated in *x*-direction by H_z according to Maxwell equation (Lorentz force is generated perpendicular to the field vectors).

Fig. 9(d) It can be distinguished between longitudinal wave and transverse waves with respect to the direction of the oscillation relative to the propagation direction. In fact the effect of H_x on transverse waves overcome the effect of H_x on longitudinal wave.

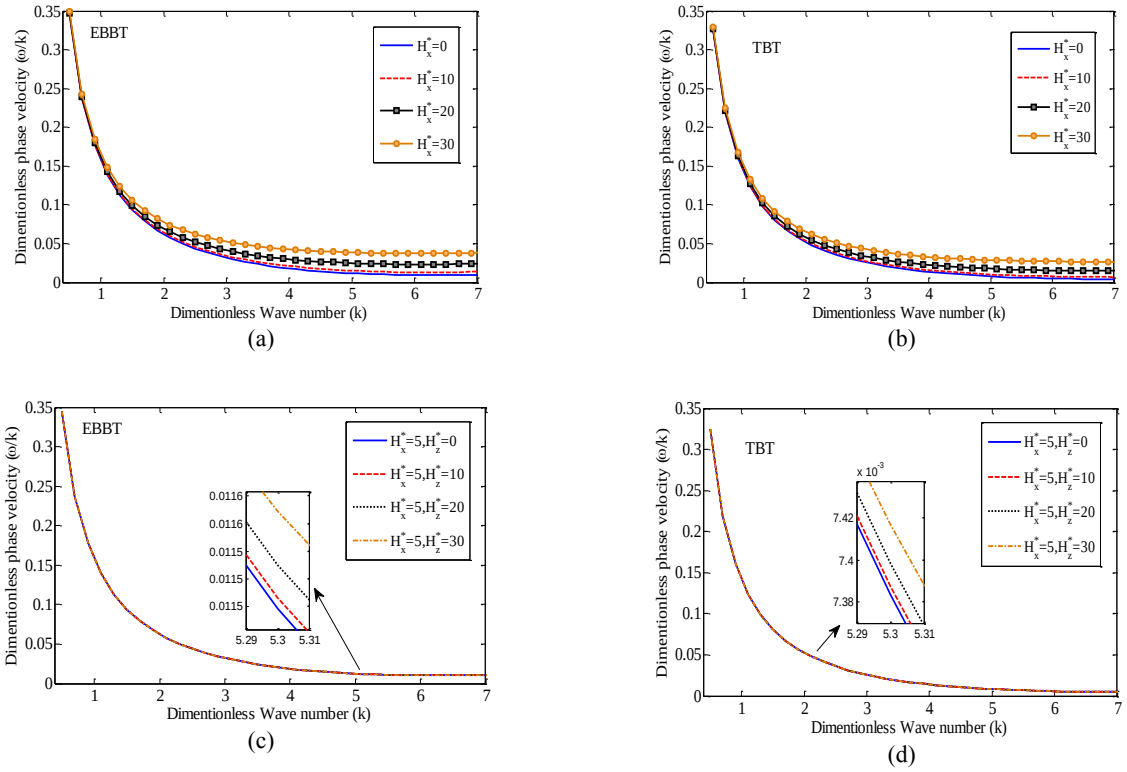

Fig.9
a) Effect of magnetic field (H_x) on dimensionless phase velocity for EBBT. b) Effect of magnetic field (H_x) on dimensionless phase velocity for TBT. c) Effect of 2D magnetic field (H_x, H_z) on dimensionless phase velocity for EBBT. d) Effect of 2D magnetic field (H_x, H_z) on dimensionless phase velocity for TBT.

10 CONCLUSIONS

Wave propagation analysis in smart polymeric nanocomposite micro-tubes reinforced by SWCNT conveying fluid was studied in this research. Visco-Pasternak foundation was utilized for modelling of elastic medium while the composite micro-tube subjected to electro-magneto-mechanical fields. The constitutive structural coefficients of nanocomposite were obtained by means of micromechanics method. The fluid flow was assumed to be incompressible, viscous and irrotational to use of Navier-Stokes equation. Micro-tube was simulated by both Euler-Bernoulli and Timoshenko beam models. Results indicated the influences of various parameters that have been listed as follows:

- Normal and shear modulus in Winkler and Pasternak models play a positive role to stability of system while damping effect lead to instability.
- The changes in the results due to change in type of fluid (density and viscosity) is negligible so that it can be ignored.
- Increasing length scale parameters in modified couple stress theory, the dimensionless phase velocity shift up. Comparison between the results show that the dimensionless phase velocity in EBBT is more than TBT.
- For both EBBT and TBT models, upstream and downstream waves join at higher wave numbers that indicate the fluid flow has no effect in the wave propagation of the higher wave number.
- When the volume fraction of fibers increase the composite become stronger, so the dimensionless phase velocity grows to higher values.
- Cutoff frequency decrease linearly and sharply with increasing dimensionless fluid velocity but the slop of changes in EBBT is lower than TBT while the first value of cutoff frequency in $u_f = 0$ is the same for both theories.

- Escape frequency decrease with increasing dimensionless fluid velocity for both EBBT and TBT where the numerical values of both models get close to each other in high fluid velocity.

This study gives physical insights which may be useful for the design and wave propagation analysis of MEMS.

ACKNOWLEDGMENTS

The author would like to thank the reviewers for their comments and suggestions to improve the clarity of this article.

REFERENCES

[1] Masuelli M.A., 2013, *Fiber Reinforced Polymers*,The Technology Applied for Concrete Repair, Argentina.
[2] Dong K., Zhu S.Q., Wang, X., 2006, Wave propagation in multiwall carbon nanotubes embedded in a matrix material, *Composite Structures* **43**(1): 194-202.
[3] Wang Q., Zhou G.Y., Lin K.C., 2006, Scale effect on wave propagation of double-walled carbon nanotubes, *International Journal of Solids and Structures* **43**(20): 6071-6084.
[4] Abdollahian M., Ghorbanpour Arani A., Mosallaie Barzoki A.A., Kolahchi R., Loghman A., 2013, Non-local wave propagation in embedded armchair TWBNNTs conveying viscous fluid using DQM, *Physica B* **418**: 1-15.
[5] Kaviani F., Mirdamadi H.Z., 2013, Wave propagation analysis of carbon nano-tube conveying fluid including slip boundary condition and strain/inertial gradient theory, *Computers and Structures* **116**: 75-87.
[6] Ghorbanpour Arani A., Kolahchi R., Vossough H., 2012, Nonlocal wave propagation in an embedded DWBNNT conveying fluid via strain gradient theory, *Physica B* **407**(21): 4281-4286.
[7] Narendar S., Gupta S.S., Gopalakrishnan S., 2012, Wave propagation in single-walled carbon nanotube under longitudinal magnetic field using nonlocal Euler–Bernoulli beam theory, *Applied Mathematical Modelling* **36**(9): 4529-4538.
[8] Ghorbanpour Arani A., Kolahchi R., Mortazavi S.A., 2014, Nonlocal piezoelasticity based wave propagation of bonded double-piezoelectric nanobeam-systems, *International Journal of Mechanics and Materials* **10**(2): 179-191.
[9] Reddy J.N., Arbind A., 2012, Bending relationships between the modified couple stress-based functionally graded Timoshenko beams and homogeneous Bernoulli–Euler beams, *Annals of Solid and Structural Mechanics* **3**(1-2):15-26.
[10] Mosallaie Barzoki A.A., Ghorbanpour Arani A., Kolahchi R., Mozdianfard M.R., Loghman A., 2013, Nonlinear buckling response of embedded piezoelectric cylindrical shell reinforced with BNNT under electro–thermo-mechanical loadings using HDQM, *Composites Part B: Engineering* **44**(1): 722-727.
[11] Tan P., Tong L., 2001, Micro-electromechanics models for piezoelectric-fiber-reinforced composite materials, *Composites Science and Technology* **61**(5): 759-769.
[12] Kuang Y.D., He X.Q., Chen C.Y., Li G.Q., 2009, Analysis of nonlinear vibrations of double walled carbon nanotubes conveying fluid, *Computational Materials Science* **45**(4): 875-580.
[13] Reddy J.N., 2002, *Energy Principles and Variational Methods in Applied Mechanics*, John Wiley, New York.
[14] Acheson D.J., 1990, *Elementary Fluid Dynamics*, Oxford Applied Mathematics and Computing Science Series, Oxford University Press.
[15] Fox R.W., McDonald A.T., Pritchard P.J., 2004, *Introduction to Fluid Mechanics*, Elsevier Ltd.
[16] Paidoussis, M.P., 1998, *Fluid-Structure Interactions*, Academic Press, California, USA.
[17] Karniadakis G., Eskok A.B., Aluru N., 2005, *Microflows and Nanoflows: Fundamentals and Simulation*, Springer.
[18] Mirramezani M., Mirdamadi H.R., 2012, The effects of Knudsen-dependent flow velocity on vibrations of a nano-pipe conveying fluid, *Archive of Applied Mechanics* **82**(7): 879-890.
[19] Ghorbanpour Arani A., Amir S., 2013, Electro-thermal vibration of visco-elastically coupled BNNT systems conveying fluid embedded on elastic foundation via strain gradient theory, *Physica B* **419**: 1-6.
[20] Kraus J., 1984, *Electromagnetics*, McGrawHill, USA.
[21] Cheng Z.Q. Lim C.W., Kitipornchai S., 2000, Three-dimensional asymptotic approach to inhomogeneous and laminated piezoelectric plates, *International Journal of Solids and Structures* **37**(23): 3153-3175.
[22] Zhang X.M., 2002, Parametric studies of coupled vibration of cylindrical pipes conveying fluid with the wave propagation approach, *Composite Structures* **80**(3-4): 287-295.
[23] Wang L., 2010, Wave propagation of fluid-conveying single-walled carbon nanotubes via gradient elasticity theory, *Computational Materials Science* **49**(4): 761-766.